IEEE Access
Multidisciplinary | Rapid Review | Open Access Journal

Received February 21, 2021, accepted March 13, 2021, date of publication April 8, 2021, date of current version April 13, 2021.

Digital Object Identifier 10.1109/ACCESS.2021.3070112

Design of a Novel Lead-Free Perovskite Solar Cell for 17.83% Efficiency

SYED ABDUL MOIZ[1], A. N. M. Alahmadi[1], AND ABDULAH JEZA ALJOHANI[2,3], (Senior Member, IEEE)

[1]Department of Electrical Engineering, Umm Al-Qura University, Makkah 21955, Saudi Arabia
[2]Department of Electrical and Computer Engineering, King Abdulaziz University, Jeddah 21589, Saudi Arabia
[3]Center of Excellence in Intelligent Engineering Systems, King Abdulaziz University, Jeddah 21589, Saudi Arabia

Corresponding author: Syed Abdul Moiz (sasyed@uqu.edu.sa)

This work was supported by the Deanship of Scientific Research at Umm Al-Qura University under Grant 18-ENG-1-01-0005.

ABSTRACT Lead halide perovskite solar cell shows an enormous potential for the next generation renewable energy, but it also offers some environmental hazards due to their inherent lead-based toxicity. On the other hand, if lead based perovskite is efficiently replaced by other non-toxic metal based perovskite then their toxicity can remarkably be reduced for photovoltaic applications. In this study, a novel lead free compound Cs_2TiBr_6 based photovoltaic device is proposed as Au/PEDOT:PSS/ Cs_2TiBr_6/TiO_2/AZO, where each layer is optimized and analysed through a series of simulations for maximum power-conversion efficiency using SCAPS-1D software. Comprehensive optimization of the thickness and doping density of each layer leads to the maximum power-conversion efficiency up to 17.83% for our proposed solar cell. Therefore, we believe that these results will provide a route heading towards the progress of lead-free and highly efficient perovskite photovoltaic devices.

INDEX TERMS Lead free, perovskite, solar-cell, numerical simulation, Cs_2TiBr_6, PEDOT:PSS, AZO, TiO_2, SCAPS 1D.

I. INTRODUCTION

Over the last few decades, researchers are very optimist about photovoltaic technology to replace the depleted fossil-fuels for enormous energy demand in near future [1]. Despite the tremendous achievements, the demands of efficient, green, low-cost, and abundantly available material for solar cell technology is a challenging task [2]. Even with the higher processing cost, the crystalline silicon is still the most dominating material and have occupied a major chunk of current photovoltaic market [3]. Up till now the laboratory power-conversion efficiency is over 25%, while the commercial power conversion-efficiency of Si solar-cell modules have reached up to 18-22% under standard testing conditions [4]–[6].

Perovskite cover a broader range of compounds with formula ABX_3, where A is an organic or inorganic cation, B is a divalent metal ion, and X is a halide anion. Perovskite solar cell has emerged as a new class with unprecedented progress and their power-conversion efficiency has already reached up to 25% within very few years [6]. It offers various advantages such as low-cost, highly-efficient, thin-film deposition, simple fabrication process, tunability of parameters including energy bandgap and excellent electrical and optical properties. However, the most efficient perovskites are lead (Pb) based compounds (e.g. methylammonium lead trihalide, $CH_3NH_3PbX_3$). Lead is inherently a toxic material and poses some serious poisonous threat to the environment which is a crucial limitation for their photovoltaic applications [7]–[10].

To replace Pb, different researchers exploring various metal ions for efficient photovoltaic solar cell. Some schools of thought are convinced that tin (Sn) can replace the Pb due to their physical and electronic similarities, however till-now Sn based perovskite solar cells did not show acceptable power-conversion efficiency [11]. Consequently, other novel divalent metal combinations are also proposed to develop efficient and stable perovskite solar cells. Wu and his co-worker reported $Cs_2AgBiBr_6$ as double perovskite solar cell [8]. Kang and his co-worker testified antioxidative stannous oxalate derived compounds for lead-free $CsSnX_3$ perovskite nanocrystals [12]. Liu et. al. has studied $CsBi_3I_{10}$ complexes to figure out efficient Pb free

The associate editor coordinating the review of this manuscript and approving it for publication was Xiao-Jun Yang.

The authors acknowledge the use of SCAPS-1D program developed by Marc Burgelman and his colleagues at the University of Gent for all the simulations reported in this work.

perovskite materials [13]. Locardi and his co-worker investigated $Cs_2AgInCl_6$ and Mn-doped $Cs_2AgInCl_6$ [14]. Ito et. al. used the mixed tin and germanium-based compound for perovskite solar cell [15]. Lefanova and his co-worker studied $(NH_4)_3Sb_2I_xBr_{9-x}$ to replace Pb for perovskite solar cell [16]. Regardless of these massive efforts, we are still far away to discover new Pb free perovskite compound which are close to methylammonium lead trihalide ($CH_3NH_3PbX_3$) with respect to efficiency and as well as stability. Recently a novel perovskite compound Cs_2TiBr_6 is reported, which shows an excellent stability response with very promising electrical and optical properties [17]–[19]. At this stage this perovskite compound is not comprehensively investigated, and little information is available, therefore wide-ranging efforts are desired [17], [18], [20].

The Cs_2TiBr_6 is inherently poly-crystalline in nature which contains many crystalline domains at different directions but separated by some grain boundaries, the average grain-boundary size can be calculated with the help of SEM and XRD analysis. The effects of poly-crystalline grain-boundary size on the performance of photovoltaic response for perovskite materials are still not very clear. Some researchers believe that the perovskite grain size plays a lesser role on the performance of perovskite solar cell as compared to the other materials parameters (e.g. tunable energy bandgaps, quantity and quality of additive, type and nature of defect density etc). Recently, researchers discovered that the grain-size of perovskite might play a crucial role for the formation of ion migration channels. These channels help the intrinsic ions to migrate from one grain to other grain boundary inside perovskite thin film at lower activation energy for switchable photovoltaic response [21].

For comprehensive investigation, different approaches are reported in literature. Among these approaches, simulation and modelling of photovoltaic devices are exceedingly popular now a day's [22]. The simulation and modelling of solar cells are based on the theoretical models which are rigorously studied and now unanimously accepted. These theoretical models can be expressed by the series of mathematical equations govern by the substantial number of physical, electrical, and optical parameters to comprehensively define the operation of associated photovoltaic material and device.

In recent literature, numerous types of both open sources software e.g. gpvdm, wxAMPS, SCAPS-1D, PC-1D, AFORS-HET, AMPS-1D etc and commercially available software such as TCAD, COMSOL, Silvaco Atlas etc are available. Among these software SCAPS-1D (Solar Cell Capacitance Simulator - 1 Dimension) is highly respected and reported for the simulation and modelling of various types of solar cell [23].

In this study we designed, proposed, and simulated Cs_2TiBr_6 based efficient perovskite solar cell. For this purpose, we select and optimized the most appropriate electron-transport layer, hole-transport layer, mesoporous layer with respect to thickness and doping concentration and then finally optimized the absorber layer (Cs_2TiBr_6) for efficient Pb free perovskite solar cell.

II. DESIGN OF NOVEL PEROVSKITE SOLAR CELL AND MATERIALS PARAMETERS

For solar cell the absorber layer is the main constituent of photovoltaic device to absorbs photons and generate electrons-hole pairs which in turn produces electricity. Theoretically, the absorber layer sandwiched between two electrodes is enough for the photovoltaic response, but the maximum photovoltaic response can only be achieved with the balanced distribution of electron and hole inside the solar cell [24]. Therefore, in order to get balanced charge distribution, the perovskite absorber is sandwiched between electron-transport layer (ETL) and hole-transport layer (HTL) for effective perovskite solar cell [25]. Where, the absorber layer we have already selected Cs_2TiBr_6 due to the reasons as discussed above.

For the selection of other layers, both HTL and ETL have to perform three well-define tasks (i) extract hole/electron from absorber layer, (ii) block opposite charges to enter from the absorber layer to avoid recombinations, and (iii) collect holes/electrons from absorber layer and guided them towards their respective electrode [26], [27]. A large number of inorganic, organic and conjugate polymers HTL materials are reported such as CuI, CuSCN, NiO, Spiro-bifluorenes, Thiophenes, Triphenylamines, Triazatruxenes, Spiro-MeOTAD, DMeO-TPD, Tetrathiafulvalene (TTF), PEDOT: PSS, P3HT, PTAA etc [26], [27]. From efficiency point of view spiro-MeOTAD has been reported as the most appropriate HTL for perovskite solar cell. But, spiro-MeOTAD has some serious issues with respect to cost, stability, compatibility, and hysteresis [28].

Broadly speaking after spiro-MeOTAD, the polymer Poly (3,4-ethylenedioxythiophene): polystyrene sulfonate (PEDOT:PSS) is the most suitable hole-transport layer candidate for efficient perovskite solar cell. PEDOT:PSS deals with many advantages of stability, low cost, excellent electrical, optical and thermal properties [29]. Therefore, we opt PEDOT:PSS as hole-transport layer for this study.

There are three structural types exist such as (i) p-i-n, (ii) n-i-p, and (iii) mesoporous type for perovskite solar cells, where both p-i-n and n-i-p are considered as planar perovskite solar cell. It is remarkably noted that compared to the plannar type, the mesoporous architecture of perovskite solar cell was found more efficient [30]. In this type, generally a mesoscopic layer is used between ETL and absorber layer and TiO_2 is the most reported mesoporous layer for perovskite solar cell [31]. As, TiO_2 behaves n-type semiconducting material in nature therefore it provides inherent support for the extraction of electrons from perovskite absorber layer. Similarly, it also supports band-alignment, and reduction of hysteresis to boost the power-conversion efficiency and stability of the perovskite solar cell [31]. Therefore, we refer TiO_2 as mesoporous layer for our proposed perovskite solar cell.

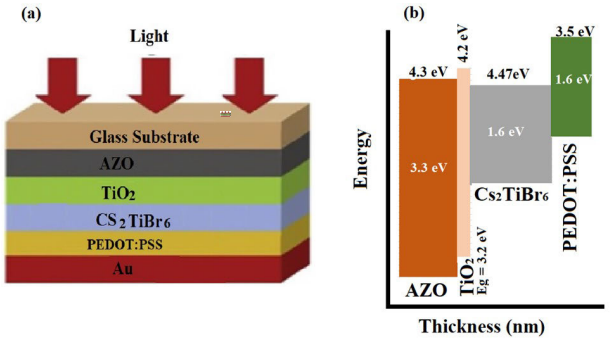

FIGURE 1. Shows (a) schematic view and (b) energy-band diagram of the proposed Au/PEDOT:PSS/Cs_2TiBr_6 /TiO_2/AZO/Glass photovoltaic device for simulation.

For ETL inorganic materials such as zinc oxide (ZnO), aluminium-doped zinc oxide (AZO), tin-oxide (SnO_2), alumina (Al_2O_3), zirconia (ZrO_2), silica (SiO_2) and many other compounds are commonly reported for perovskite solar cell. Among these electron-transport materials, ZnO has many unique advantages of solution processing, excellent electrical properties and high mobility. However, frequent instabilities and poor device efficiency of perovskite solar cell with ZnO have already reported [32]. By using Al doped ZnO for electron-transport layer, excellent photovoltaic response and stability can be achieved due to improved conductivity, better work-function alignment, and acid resistance [33]. Therefore, in this study we prefer AZO (n-ZnO:Al) as electron-transport layer. Figure 1 shows the both (a) schematic and (b) energy band diagram of the proposed device used in this study as Au/PEDOT:PSS/Cs_2TiBr_6/TiO_2/AZO perovskite solar cell.

III. SIMULATION, MODELLING AND DESIGN PARAMETERS

As discussed above, the simulation in this study is employed with the help of SCAPS software version 3.3.07 which was developed by ELIS, University of Gent, Belgium and it is a one dimension (1-D) photovoltaic simulator [23]. The SCAPS software is versatile in nature and covers nearly all recommended electrical, optical and photovoltaic models, therefore it can be successfully used for the simulation of dye-sensitized solar cell [34], [35], graphene [36], CIGS materials [37], polymer [38], nanowire [39], perovskite and many other types of photovoltaic materials [40]. Kang et. al. reported the simulation analysis of graphene contact for perovskite solar cell [41]. Abdelaziz comprehensively investigated and reported the performance of tin-based perovskite solar cell by SCAPS device simulation [42]. On the other hand, the reasonable agreements of the experimental findings with SCAPS-1D simulation results [43], inspired us to use this open-source software for this work.

Fundamentally, SCAPS 1D execute four set of photovoltaic equations for both electron and hole carriers density separately [44]. These equations are

1) Poisson equation:

$$\frac{d^2\phi(x)}{dx^2} = \frac{e}{\varepsilon_0\varepsilon_r}\left(p(x) - n(x) + N_D - N_A + \rho_p - \rho_n\right), \tag{1}$$

where ϕ is the is the electrostatics potential, e is electronic charge, ε_0 is permittivity of vacuume, ε_r is relative permittivity, N_D is the shallow donor impurity density and N_A is the shallow acceptor impurity density. Similarly ρ_p is hole density distribution and ρ_n is the electrons density distribution, while n(x) and p(x) are the the electron and hole density as a function of x respectively.

2) Continuity equation:

$$\frac{dJ_n}{dx} = G - R \tag{2}$$

$$\frac{dJ_p}{dx} = G - R \tag{3}$$

where J_n and J_p are the electron and hole current densities, G is the generation rate and R is the recombination rate.

3) Charge transport equation:

$$J_n = D_n\frac{dn}{dx} + \mu_n n\frac{d\phi}{dx} \tag{4}$$

$$J_p = D_p\frac{dp}{dx} + \mu_p p\frac{d\phi}{dx} \tag{5}$$

where D_n and D_p are the electron and hole diffusion coefficient respectively, μ_n and μ_p are the electron and hole mobility respectively.

4) Absorption coefficient equation: For the determination of the absorption coefficient $\alpha(\lambda)$, we use the following equation

$$\alpha(\lambda) = \left(A + \frac{B}{h\nu}\right)\sqrt{h\nu - E_g} \tag{6}$$

where A, B are constant, h is plank constant, ν is frequency of photons and E_g is the band gap of the absorber layer.

The band discontinuity between the interface of the different layers is presumed small and therefore can be neglected for simplicity. The ambient temperature 300 K and the solar spectrum AM.1.5 (1000 W/m^2) is used for this study. All physical and electrical parameters which are required by SCAPS 1D for each layer are extracted from scientific literature and are listed above in Table 1.

IV. RESULTS AND DISCUSSION

A. PEDOT: PSS THICKNESS OPTIMIZATION

The charge-transport process in PEDOT:PSS is not so efficient and offers high resistance in the presence of low conductive PSS contents [45]–[47]. Therefore, in order to simulate high resistive PEDOT:PSS we introduced some interface defects and detailed information can be found from Table 2. To optimize the PEDOT:PSS for this study, firstly

TABLE 1. Photovoltaic device parameters used for these simulations are reported here, where doping concentration are just given for initial estimation which are optimized in later stages.

photovoltaic Parameters	Symbol	Unit	PEDOT:PSS	AZO	TiO_2	Cs_2TiBr_6
Energy Bandgap	Eg	eV	1.6	3.3	3.2	1.6
Electron Affinity	χ	eV	3.5	4.3	4.2	4.47
Dielectric Permittivity (Relative)	ε	-	3	9	10	10
Effective Density of Stated at Valence Band	N_v	cm^{-3}	1.00E+22	1.80E+18	1.80E+18	1.00E+19
Effective Density of Stated at Conduction Band	NC	cm^{-3}	1.00E+22	2.20E+18	2.20E+18	1.00E+19
Hole Thermal Velocity	Ve	cm/sec	1.00E+07	1.00E+07	1.00E+07	1.00E+07
Electron Thermal Velocity	Vh	cm/sec	1.00E+07	1.00E+07	1.00E+07	1.00E+07
Hole Mobility	μ_h	cm^2/V.sec	9.90E-05	2.50E+01	2.50E+01	2.50E00
Electron Mobility	μ_e	cm^2/V.sec	4.50E-04	2.00E+02	1.00E+02	4.40E+01
Uniform Shallow Acceptor Dopping	Na	cm^{-3}	1.00E+18	0	0	0
Uniform Shallow Donor Dopping	Nd	cm^{-3}	0	1.00E+14	1.00E+11	1.00E+13

TABLE 2. Defect interface parameters between PEDOT:PSS and $Cs_2T_iBr_6$ absorber.

Parameters	Unit	Values
Defect Type	–	Neutral
Capture cross section for electron	cm^{-3}	1.00E+14
Capture cross section for hole	cm^{-3}	1.00E+14
Energetic Distribution	–	Single
Energy level with respect to Ev	eV	6.00E-01
Characteristic Energy	eV	approx. 0.1
Defect Density	cm^{-3}	4.50E+17

we optimized the thickness and then acceptor doping density for PEDOT:PSS layer. For this purpose, initially we used the Table 1 parameters and run the software for proposed device and obtained results are shown in Figure 2 and Figure 3, respectively.

Film-thickness of PEDOT:PSS as HTL plays a vital role to define the photovoltaic efficiency of the solar cell since it interacts with both perovskite absorber layer and anode material to handle charge collection, charge recombination and hopping charge transport processes at the same time. In order to determine the optimized thickness of PEDOT:PSS, the illuminated current-voltage simulation of the proposed solar cell were carries out and the photovoltaic parameters such as (a) open-circuit voltage, (b) short-circuit current, (c) fill-factor and (d) power-conversion efficiency were calculated as a function of film-thickness from 10 to 100 nm and the results are shown in Figure 2a and 2b. From the figures it is clearly observed that both short-circuit voltage and fill-factor are initially increases and reaching maximum at 80 nm PEDOT:PSS thickness and are started to decreases, while open-circuit voltage behaves oppositely but within very small scale. PEDOT:PSS contributes two types of recombination, (i) interface recombination and (ii) volume bulk recombination, both are function of film-thickness. At higher film-thickness surface recombination dominate to degrade open circuit voltage [48]. As power-conversion efficiency is the resultant of all these factors, so it rises and reaches maximum (6.47%) at 80 nm and then start to decreases as a function

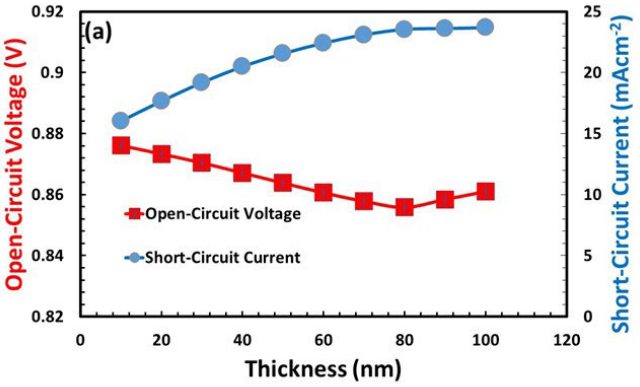

(a) Short-circuit current ($mAcm^{-2}$) and open-circuit voltage (Volts)

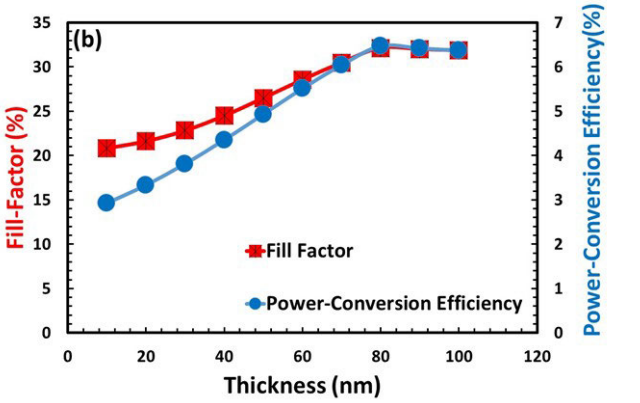

(b) Fill-factor (%) and power-conversion efficiency (%) as a function of PEDOT:PSS film thickness.

FIGURE 2. Simulated device parameters.

of PEDOT:PSS layer thickness. Like many other conducting polymers, the charge transportation and recombination are very complex in nature and specially in the presence of traps distribution [49]–[53], so we can infer that all these factors are optimized at 80 nm thickness of PEDOT:PSS for our proposed solar cell.

B. PEDOT: PSS ACCEPTOR DENSITY OPTIMIZATION

Despite the numerous advantages, PEDOT: PSS shows inherently low conductivity and therefore the doping of PEDOT:PSS is essential for efficient photovoltaic applications. Doping is generally performed by introducing suitable amount of some compounds into the PEDOT:PSS aqueous solution, such compounds may be ionic, polar, organic, polymer anionic, and surfactant compounds. The conductivity of PEDOT:PSS can be further enhanced from two to three orders of magnitude by using proper doping compound under normal conditions [54]. It is experimentally noted that the successful doping beyond 10^{20} cm^{-3} is not a conventional task and the conductivity of both organic semiconductor and inorganic semiconductor increase with doping up to a certain limit (10^{20} cm^{-3}) and then start to decrease [55]. It may be due to the carrier-carrier or may be carrier-molecular orbital interactions, therefore in this study we

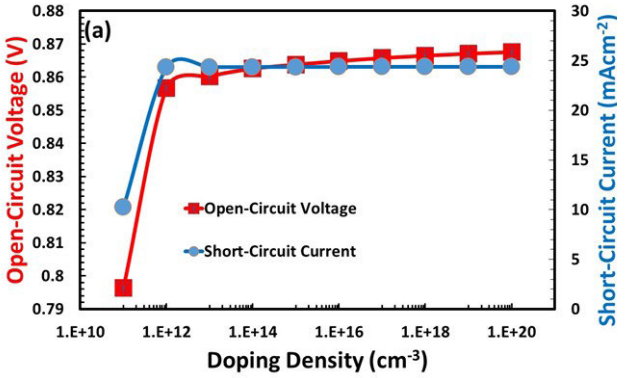

(a) Short-circuit current (mAcm^{-2}), and open-circuit voltage (Volts

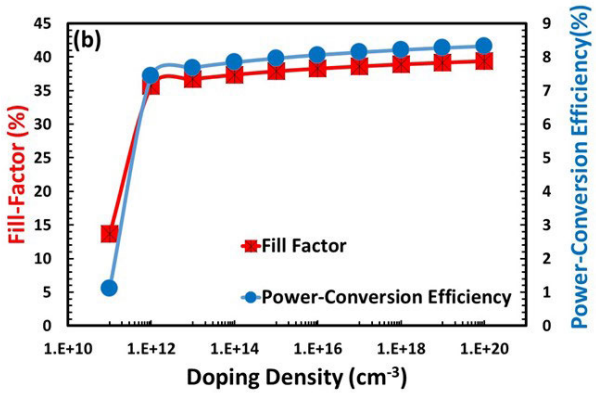

(b) Fill-factor (%) and power-conversion efficiency (%) as a functio of PEDOT:PSS shallow acceptor doping density.

FIGURE 3. Simulated device parameters.

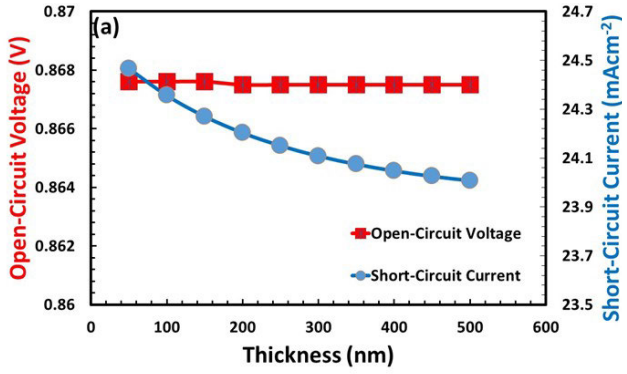

(a) Short-circuit current (mAcm^{-2}) and open-circuit voltage (Volts).

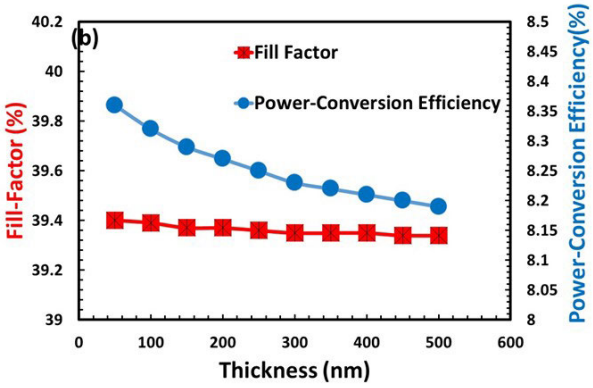

(b) Fill-factor (%) and power-conversion efficiency (%) as a function of AZO thin film thickness.

FIGURE 4. Simulated device parameters.

analysed the photovoltaic response of ETL, HTL and meso-porous layer for our proposed device up to 10^{20} cm^{-3} doping concentration [56].

In Figure 3a and 3b, firstly incorporated the optimize thickness of PEDOT:PSS (80 nm) and then we varied the shallow acceptor doping density (Na) inside by PEDOT:PSS from 10^{11} to 10^{20} cm^{-3} and different photovoltaic parameters such as (a) short-circuit current, open-circuit voltage, (b) fill-factor and power-conversion efficiency were calculated from the photovoltaic responses. Figures 3a and 3b demonstrate the similar trends, where open-circuit voltage, short-circuit current, and fill-factor are firstly increases sharply and then gradually increases. Similarly, the power-conversion efficiency is also increases sharply and then steadily with doping concentration and the maximum efficiency close to 8.3% is observed at most optimum doping 10^{20} cm^{-3} for PEDOT:PSS for our proposed solar cell.

C. AZO THICKNESS OPTIMIZATION

The aluminium doped ZnO (AZO) plays two types of role, one as electron-transport layer and other as a transparent conductive oxide (TCO) for photovoltaic response, therefore their optimization is also very important for efficient solar cell. For thickness optimization, the photovoltaics parameters such as (a) open-circuit voltage, (b) short-circuit current, (c) fill-factor and (d) power- conversion efficiency of Au/PEDOT:PSS/Cs_2TiBr_6/TiO_2/AZO solar cell were examined by varying AZO layer's thickness from 100 to 500 nm and the results are summarized in Figure 4a and 4b respectively. We observed that the effects of thickness on open-circuit voltage is nearly negligible, while short-circuit current rises up to 400 nm and then start to decrease. Similarly, Fill-factor is continuously decreases with AZO thickness and power-conversion efficiency is very slightly decreases with AZO layer thickness. So on the basis of the results we can conclude that 100 nm (PCE 8.37%) is the most optimum thickness of AZO layer for efficient Au/PEDOT:PSS/Cs_2TiBr_6/TiO_2/AZO solar cell.

D. AZO DONOR DENSITY OPTIMIZATION

The conductivity of AZO (n-ZnO:Al) is not comparable with other transparent conductive oxides (TCO) such as indium tin oxide (ITO) and fluorine tin oxide (FTO), which are frequently used for perovskite solar cell [57]. But the conductivity (σ, which is the inverse of resistivity $\rho = \frac{1}{en\mu}$) can be increased by either increasing mobility and/or increasing free electron density. Doping is the easiest way to increase the free electron carrier density, but on the other side heavy doping degrades optical absorption, reflection and transmission

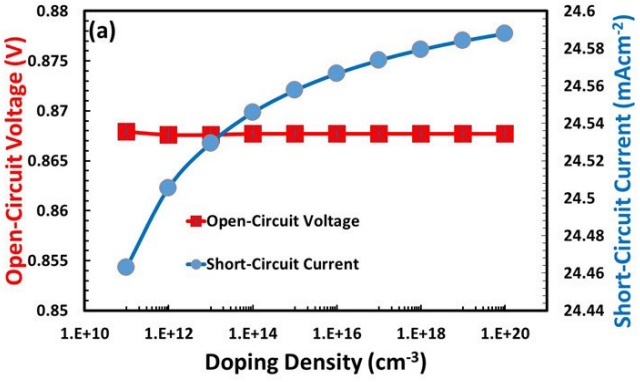

(a) Short-circuit current and open-circuit voltage

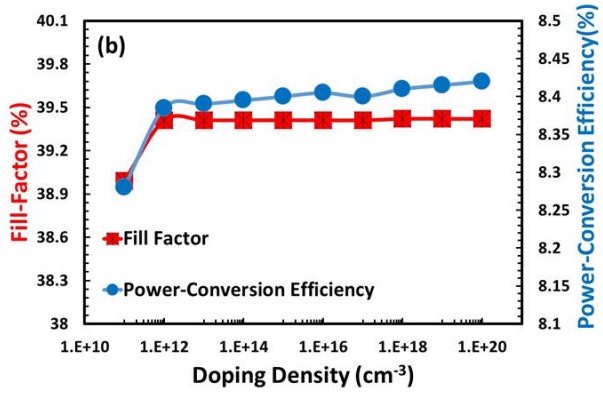

(b) Fill-factor (%) and power-conversion efficiency (%) as a function of AZO donor density optimization.

FIGURE 5. Simulated device parameters.

for photovoltaic response. Similarly, higher donor doping can also degrade the electron mobility and hence it is very important to optimize the donor doping of AZO for highly optimized solar cell [58], [59].

For donor doping-density, the photovoltaics parameters such as (a) open-circuit voltage, (b) short-circuit current, (c) fill-factor and (d) power-conversion efficiency of Au/PEDOT:PSS/Cs_2TiBr_6/TiO_2/AZO solar cell were examined by varying shallow donor doping from 10^{11} to 10^{20} cm^{-3} of AZO layer and the results are shown in Fig. 5a and 5b respectively. It is realized that all photovoltaic parameters are improved by doping concentration but with different rates. Short-circuit current is significantly increases while open-circuit voltage is nearly unaffected with increasing doping concentration. Power-conversion efficiency and fill-factor are sharply increased at early stage (up to 10^{12} cm^{-3}) and then increases very slightly. So, the optimum efficiency (8.42 %) of the device is achieved at the donor density of 10^{20} cm^{-3} respectively.

E. TiO_2 THICKNESS OPTIMIZATION

The TiO_2 interaction with perovskite material is complex in nature and offers some unique behaviour such as high chemical reactivity, unwanted charge build-up, excessive recombination, and uncertainty under ultraviolet light, low mobility, non-uniform distribution of electronic trap states, and high density of these trap states [60].

Generally, it can be observed by both theoretically (e.g. DFT: density functional theory) and experimentally (e.g. XPS: X-ray photo-electron spectroscopy) that the inorganic perovskite material such as Cs_2TiBr_6 offers a weak interface with inorganic metal oxide layer (e,g TiO_2, ZnO etc) leading towards low power conversion efficiency. Such weaker contact is formed due to the non-existence of hydrogen bonds during the interfacial chemical reactions between metal oxide and perovskite layers compared to the organic-perovskite interfaces. Therefore, numerous organic additives are reported for the formation of strong hydrogen bonding to improve the interfacial contact between perovskite and inorganic metal oxide layer but at the cost of thermal stability and hysterics for perovskite solar cell.

The photovoltaic parameter responses of the device are simulated when TiO_2 film thickness is varied from 10 to 100 nm as shown in Figure 6a and 6b respectively. Figure 6a shows the open-circuit voltage and short-circuit current behaviours as a function of TiO_2 film thickness. It is clear from the figure that the open-circuit voltage is very slightly increases (nearly constant), while short-circuit current of the device is very slightly decreases (nearly constant) as a function of TiO_2 film thickness, respectively. Similarly, Figure 6b shows the fill-factor and power-conversion efficiency response as a function of TiO_2 film thickness. It is also evident from the figure that the fill-factor's behaviour is very similar to short-circuit current, while power-conversion efficiency of the device is linearly decreases as a function of TiO_2 film thickness and maximum value is observed at 8.45% for 20 nm TiO_2 film thickness, respectively. As power-conversion efficiency is the prime parameter, therefore we can infer that the most optimum thickness of TiO_2 for proposed device is 20 nm.

F. TiO_2 DOPING OPTIMIZATION

Similarly, we also analysed the proposed device to determine the optimum donor density for TiO_2 layer. Very similar results for (i) open-circuit voltage, (ii) short circuit Current, (iii) fill-factor and (iv) power-conversion efficiency are observed as already shown in Figure 6. It is also noted that the maximum power-conversion efficiency 9.18% is achieved at donor doping 10^{12} cm^{-3} for TiO_2 layer. Therefore, the TiO_2 doping density effects on photovoltaic responses are not shown here for simplicity.

G. THE ABSORBER Cs_2TiBr_6 THICKNESS OPTIMIZATION

After incorporating the optimized thickness and doping density of PEDOT:PSS as hole-transport layer, TiO_2 as mesoporous layer and AZO as electron-transport layer, we are finally interested to determine the most optimum power-conversion efficiency of our proposed device. As we know that the power-conversion efficiency is related to the thickness of Cs_2TiBr_6 absorber layer, therefore we analysed the photovoltaic parameters of the proposed device as a

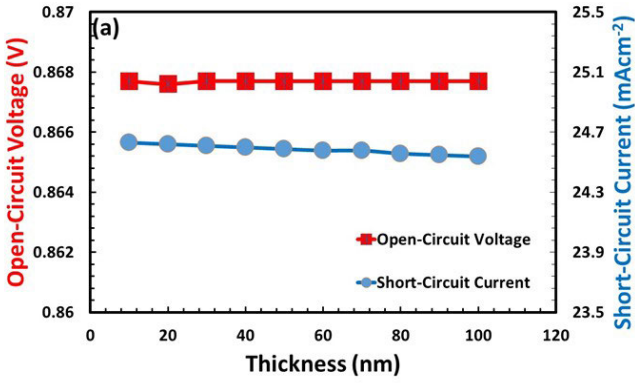

(a) Short-circuit current and open-circuit voltage.

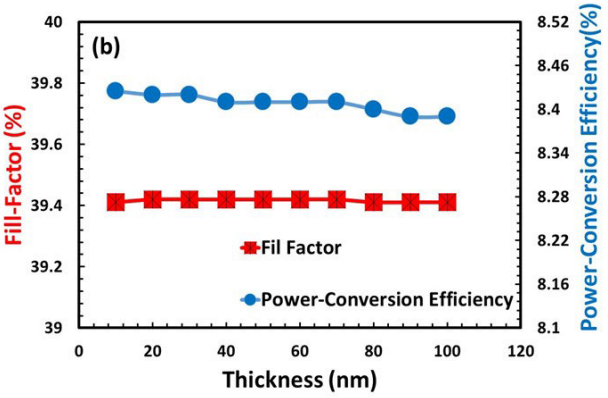

(b) Fill-factor (%) and power-conversion efficiency (%) as a function of TiO_2 film thickness.

FIGURE 6. Simulated device parameters.

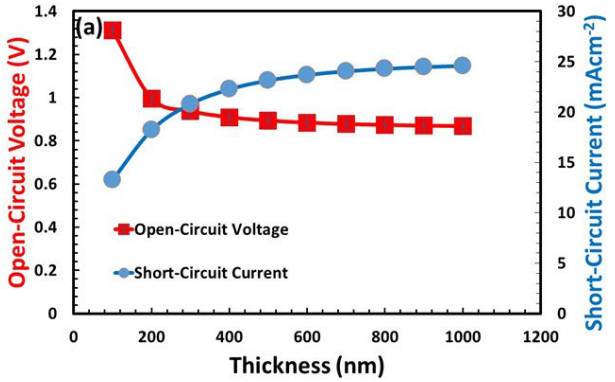

(a) Short-circuit current and open-circuit voltage.

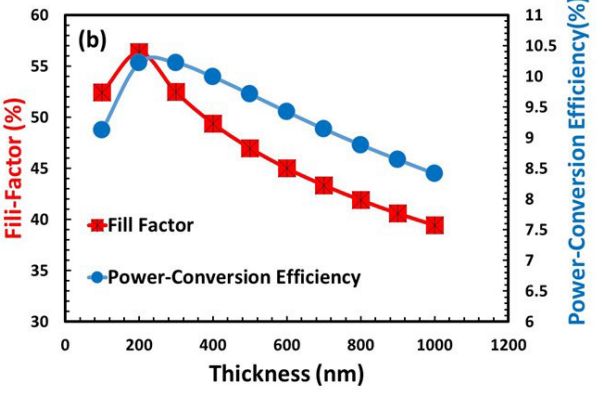

(b) Fill-factor (%) and power-conversion efficiency (%) as a function of Cs_2TiBr_6 layer thickness.

FIGURE 7. Simulated device parameters.

function of Cs_2TiBr_6 layer thickness from 100 to 1000 nm and the results are given in Figure 7a and 7b respectively. In Figure 7a, it is observed that the short-circuit current is continuously increased but at later stage the rate of increment is very slow as a function of perovskite absorber layer thickness. As perovskite absorber thickness increases then more optical absorption can be taken place which in turn leads to the higher electron-hole pair generation and therefore short-circuit current is constantly increases as shown in Figure 7a. On the other hand, open-circuit voltage is sharply dropped from 1.3 V to 1 V and then slightly decreases as the thickness increases of the absorber layer. Such open-circuit voltage losses in the proposed solar cell may be due to the accumulation of positive hole charges at the interface with Cs_2TiBr_6 absorber layer as similar observations were already reported by many other studies [61]–[63]. Accumulation of interfacial charges causes to enhance charge carrier recombination and hence a significant drop of open-circuit voltage is observed.

Accumulation of interfacial charges also effects fill-factor and power-conversion efficiency as shown in Figure 7b. Therefore, more or less similar power-conversion efficiency and fill-factor responses are observed as both increase significantly at early stage and reached maximum value (power-conversion efficiency 10.62%) at 200 nm thickness then very steadily decreases with increasing absorber layer thickness. It may be the trade of balance between generation of free carriers, and interfacial recombination as a function of absorber layer thickness. Hence, based on these results and specially power-conversion efficiency we can infer that the best thickness is 200 nm for Cs_2TiBr_6 absorber layer for our proposed solar device.

H. THE ABSORBER Cs_2TiBr_6 DOPING OPTIMIZATION

The presence of inherent interfacial traps states of perovskite material causes to accumulate unwanted charge carriers which in turn trigger excessive recombination to degrade the photovoltaic response [64]. Perovskite materials are polycrystalline in nature and also have non-uniform bulk distribution of trap states, which further worsen the photovoltaic response of perovskite solar cell. As discussed above the doping is one of the most effective and easy solution to fill their surface traps, minimize unwanted charge accumulation and significantly enhance the electron injection efficiency to improve the photovoltaic response of perovskite solar cell [65], [66]. In order to determine the optimum doping density, the photovoltaic parameters of the proposed device are investigated by varying the absorber doping density from 10^{11} to 10^{20} cm^{-3} and the results are summarized in Figure 8a and 8b respectively. From the both Figures it is observed that the open-circuit voltage, short-circuit

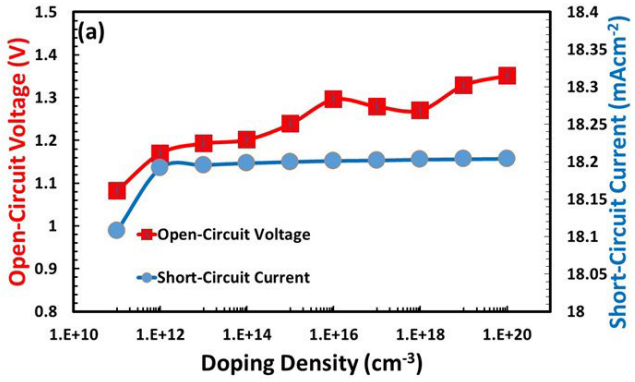

(a) Short-circuit current and open-circuit voltage.

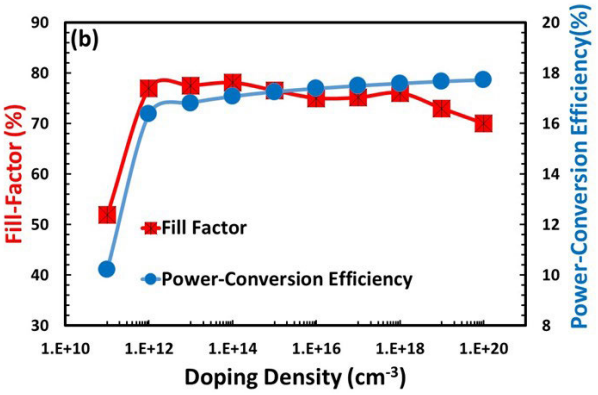

(b) Fill-factor (%) and power-conversion efficiency (%) as a function of Cs_2TiBr_6 doping density.

FIGURE 8. Simulated device parameters.

TABLE 3. The optimized photovoltaic parameters for each layer for proposed device Al/PEDOT:PSS/Cs_2TiBr_6/TiO_2/AZO/Glass determine from the series of simulations.

Solar Cell Proposed Layers	Thickness L(nm)	Donor Doping Density $N_D(cm^{-3})$	Acceptor Doping Density $N_A(cm^{-3})$
PEDOT:PSS	80	0	1.00E+20
AZO	100	1.00E+20	0
TiO_2	20	1.00E+12	0
$Cs_2T_iBr_6$	200	1.00E+20	0

current, and power-conversion efficiency of the proposed device are continuously increasing with shallow donor doping and power-conversion efficiency reached up to 17.83 % at 10^{20} cm^{-3} doping of Cs_2TiBr_6 absorber layer respectively. At higher doping the fill-factor follows complex response which may be due to higher leakage current at heavy doping [67]. Thus, the optimum doping of absorber layer is 10^{20} cm^{-3} for the most efficient design of proposed solar cell.

Finally, we figure out the most optimum thickness and doping parameters of each layer of our proposed solar cell and listed in Table 3. As Cs_2TiBr_6 is a novel perovskite material for photovoltaic response and little information is available in literature, therefore we compared our proposed photovoltaic device with other Cs_2TiBr_6 based reported solar cell and it is found that the maximum power-conversion efficiency of our proposed solar cell is improved from 3% to 17.83% mainly due to the proper material selection, thickness and doping concentration of hole-transport, electron-transport, mesoporous and perovskite absorber layer [17]–[20].

V. CONCLUSION

In this study we firstly designed novel Cs_2TiBr_6 based photovoltaic device according to the available literature information. We proposed highly suitable hole-transport layer (PEDOT:PSS), mesoporous layer (TiO_2) and electron-transport layer (AZO) as Au/PEDOT:PSS/Cs_2TiBr_6/TiO_2/AZO, and simulated by SCAPS-1D software. To improve the power-conversion efficiency of the proposed lead-free perovskite solar cell, an effort has been made by optimizing the hole-transport layer, electron transport layer, mesoporous layer and then Cs_2TiBr_6 absorber layer. After comprehensive optimization of each layer thickness, and doping density the maximum 17.83% power-conversion efficiency is achieved for the proposed device. It is further observed that the photovoltaic parameters of the perovskite solar-cell are significantly affected by the thickness and doping concentration of respective hole-transport layer, electron transport layer, and perovskite absorber layer. Therefore, not only the proper selection of materials but also the thickness and doping concentration play a vital role for an efficient perovskite solar cell. The overall outcomes of this study will not only help to understand the photovoltaic process but also provide a route heading towards the progress of lead-free and highly efficient photovoltaic devices.

ACKNOWLEDGMENT

The authors would like to thank the Deanship of Scientific Research at Umm Al-Qura University for supporting this work by Grant Code: 18-ENG-1-01-0005.

REFERENCES

[1] E. Kabir, P. Kumar, S. Kumar, A. A. Adelodun, and K.-H. Kim, "Solar energy: Potential and future prospects," *Renew. Sustain. Energy Rev.*, vol. 82, pp. 894–900, Feb. 2018.

[2] S. Almosni, A. Delamarre, Z. Jehl, D. Suchet, L. Cojocaru, M. Giteau, B. Behaghel, A. Julian, C. Ibrahim, L. Tatry, and H. Wang, "Material challenges for solar cells in the twenty-first century: Directions in emerging technologies," *Sci. Technol. Adv. Mater.*, vol. 19, no. 1, pp. 336–369, 2018.

[3] E. Płaczek-Popko, "Top PV market solar cells 2016," *Opto-Electron. Rev.*, vol. 25, no. 2, pp. 55–64, Jun. 2017.

[4] M. A. Green, "The path to 25% silicon solar cell efficiency: History of silicon cell evolution," *Prog. Photovolt., Res. Appl.*, vol. 17, no. 3, pp. 183–189, May 2009.

[5] S. Gharibzadeh, I. M. Hossain, P. Fassl, B. A. Nejand, T. Abzieher, M. Schultes, E. Ahlswede, P. Jackson, M. Powalla, S. Schäfer, M. Rienäcker, T. Wietler, R. Peibst, U. Lemmer, B. S. Richards, and U. W. Paetzold, "2D/3D heterostructure for semitransparent perovskite solar cells with engineered bandgap enables efficiencies exceeding 25% in four-terminal tandems with silicon and CIGS," *Adv. Funct. Mater.*, vol. 30, no. 19, May 2020, Art. no. 1909919.

[6] M. Jeong, I. W. Choi, E. M. Go, Y. Cho, M. Kim, B. Lee, S. Jeong, Y. Jo, H. W. Choi, J. Lee, and J. H. Bae, "Stable perovskite solar cells with efficiency exceeding 24.8% and 0.3-V voltage loss," *Science*, vol. 369, no. 6511, pp. 1615–1620, 2020.

[7] A. Bibi, I. Lee, Y. Nah, O. Allam, H. Kim, L. N. Quan, J. Tang, A. Walsh, S. S. Jang, E. H. Sargent, and D. H. Kim, "Lead-free halide double perovskites: Toward stable and sustainable optoelectronic devices," *Mater. Today*, Jan. 2021.

[8] C. Wu, Q. Zhang, Y. Liu, W. Luo, X. Guo, Z. Huang, H. Ting, W. Sun, X. Zhong, S. Wei, and S. Wang, "The dawn of lead-free perovskite solar cell: Highly stable double perovskite $Cs_2AgBiBr_6$ film," *Adv. Sci.*, vol. 5, no. 3, 2018, Art. no. 1700759.
[9] Y. Yang and J. You, "Make perovskite solar cells stable," *Nature News*, vol. 544, no. 7649, p. 155, 2017.
[10] J. Wang, J. Dong, F. Lu, C. Sun, Q. Zhang, and N. Wang, "Two-dimensional lead-free halide perovskite materials and devices," *J. Mater. Chem. A*, vol. 7, no. 41, pp. 23563–23576, 2019.
[11] W. Ke and M. G. Kanatzidis, "Prospects for low-toxicity lead-free perovskite solar cells," *Nature Commun.*, vol. 10, no. 1, pp. 1–4, Dec. 2019.
[12] C. Kang, H. Rao, Y. Fang, J. Zeng, Z. Pan, and X. Zhong, "Antioxidative stannous oxalate derived lead-free stable $CsSnX_3$ (X=Cl, Br, and I) perovskite nanocrystals," *Angew. Chem.*, vol. 133, no. 2, pp. 670–675, Jan. 2021.
[13] Z. Liu, S. Dai, Y. Wang, B. Yang, D. Hao, D. Liu, Y. Zhao, L. Fang, Q. Ou, S. Jin, J. Zhao, and J. Huang, "Photoresponsive transistors based on lead-free perovskite and carbon nanotubes," *Adv. Funct. Mater.*, vol. 30, no. 3, Jan. 2020, Art. no. 1906335.
[14] F. Locardi, M. Cirignano, D. Baranov, Z. Dang, M. Prato, F. Drago, M. Ferretti, V. Pinchetti, M. Fanciulli, S. Brovelli, L. De Trizio, and L. Manna, "Colloidal synthesis of double perovskite $Cs_2AgInCl_6$ and Mn-doped $Cs_2AgInCl_6$ nanocrystals," *J. Amer. Chem. Soc.*, vol. 140, no. 40, pp. 12989–12995, Oct. 2018.
[15] N. Ito, M. A. Kamarudin, D. Hirotani, Y. Zhang, Q. Shen, Y. Ogomi, S. Iikubo, T. Minemoto, K. Yoshino, and S. Hayase, "Mixed Sn–Ge perovskite for enhanced perovskite solar cell performance in air," *J. Phys. Chem. Lett.*, vol. 9, no. 7, pp. 1682–1688, 2018.
[16] A. Iefanova, N. Adhikari, A. Dubey, D. Khatiwada, and Q. Qiao, "Lead free $CH_3NH_3SnI_3$ perovskite thin-film with p-type semiconducting nature and metal-like conductivity," *AIP Adv.*, vol. 6, no. 8, Aug. 2016, Art. no. 085312.
[17] J. Euvrard, X. Wang, T. Li, Y. Yan, and D. B. Mitzi, "Is Cs_2TiBr_6 a promising pb-free perovskite for solar energy applications?" *J. Mater. Chem. A*, vol. 8, no. 7, pp. 4049–4054, 2020.
[18] K. Chakraborty, M. G. Choudhury, and S. Paul, "Numerical study of Cs_2TiX_6 (X=Br−, I−, F− and Cl−) based perovskite solar cell using SCAPS-1D device simulation," *Sol. Energy*, vol. 194, pp. 886–892, Dec. 2019.
[19] M. R. Jani, M. T. Islam, S. M. Al Amin, M. S. Us Sami, K. M. Shorowordi, M. I. Hossain, S. Chowdhury, S. S. Nishat, and S. Ahmed, "Exploring solar cell performance of inorganic Cs_2TiBr_6 halide double perovskite: A numerical study," *Superlattices Microstructures*, vol. 146, Oct. 2020, Art. no. 106652.
[20] M. Chen, M.-G. Ju, A. D. Carl, Y. Zong, R. L. Grimm, J. Gu, X. C. Zeng, Y. Zhou, and N. P. Padture, "Cesium titanium (IV) bromide thin films based stable lead-free perovskite solar cells," *Joule*, vol. 2, no. 3, pp. 558–570, Mar. 2018.
[21] W. Zhou, J. Gu, Z. Yang, M. Wang, and Q. Zhao, "Basis and effects of ion migration on photovoltaic performance of perovskite solar cells," *J. Phys. D, Appl. Phys.*, vol. 54, no. 6, Feb. 2021, Art. no. 063001.
[22] P. P. Altermatt, "Models for numerical device simulations of crystalline silicon solar cells—A review," *J. Comput. Electron.*, vol. 10, no. 3, pp. 314–330, Sep. 2011.
[23] M. Burgelman, P. Nollet, and S. Degrave, "Modelling polycrystalline semiconductor solar cells," *Thin Solid Films*, vols. 361–362, pp. 527–532, Feb. 2000.
[24] K. Chen, Q. Hu, T. Liu, L. Zhao, D. Luo, J. Wu, Y. Zhang, W. Zhang, F. Liu, T. P. Russell, R. Zhu, and Q. Gong, "Charge-carrier balance for highly efficient inverted planar heterojunction perovskite solar cells," *Adv. Mater.*, vol. 28, no. 48, pp. 10718–10724, Dec. 2016.
[25] A. A. Said, J. Xie, and Q. Zhang, "Recent progress in organic electron transport materials in inverted perovskite solar cells," *Small*, vol. 15, no. 27, Jul. 2019, Art. no. 1900854.
[26] S. Pitchaiya, M. Natarajan, A. Santhanam, V. Asokan, A. Yuvapragasam, V. M. Ramakrishnan, S. E. Palanisamy, S. Sundaram, and D. Velauthapillai, "A review on the classification of organic/inorganic/carbonaceous hole transporting materials for perovskite solar cell application," *Arabian J. Chem.*, vol. 13, no. 1, pp. 2526–2557, Jan. 2020.
[27] P.-Y. Gu, N. Wang, A. Wu, Z. Wang, M. Tian, Z. Fu, X. W. Sun, and Q. Zhang, "An azaacene derivative as promising electron-transport layer for inverted perovskite solar cells," *Chem.-Asian J.*, vol. 11, no. 15, pp. 2135–2138, Aug. 2016.
[28] Z. Hawash, L. K. Ono, and Y. Qi, "Recent advances in spiro-MeOTAD hole transport material and its applications in organic–inorganic halide perovskite solar cells," *Adv. Mater. Interface*, vol. 5, no. 1, Jan. 2018, Art. no. 1700623.
[29] L. Hu, M. Li, K. Yang, Z. Xiong, B. Yang, M. Wang, X. Tang, Z. Zang, X. Liu, B. Li, and Z. Xiao, "PEDOT:PSS monolayers to enhance the hole extraction and stability of perovskite solar cells," *J. Mater. Chem. A*, vol. 6, no. 34, pp. 16583–16589, 2018.
[30] D. Ramirez, K. Schutt, J. F. Montoya, S. Mesa, J. Lim, H. J. Snaith, and F. Jaramillo, "Meso-superstructured perovskite solar cells: Revealing the role of the mesoporous layer," *J. Phys. Chem. C*, vol. 122, no. 37, pp. 21239–21247, Sep. 2018.
[31] B. Parida, A. Singh, M. Oh, M. Jeon, J.-W. Kang, and H. Kim, "Effect of compact TiO_2 layer on structural, optical, and performance characteristics of mesoporous perovskite solar cells," *Mater. Today Commun.*, vol. 18, pp. 176–183, Mar. 2019.
[32] K. Schutt, P. K. Nayak, A. J. Ramadan, B. Wenger, Y.-H. Lin, and H. J. Snaith, "Overcoming zinc oxide interface instability with a methylammonium-free perovskite for high-performance solar cells," *Adv. Funct. Mater.*, vol. 29, no. 47, 2019, Art. no. 1900466.
[33] K. Wang, S. Olthof, W. S. Subhani, X. Jiang, Y. Cao, L. Duan, H. Wang, M. Du, and S. F. Liu, "Novel inorganic electron transport layers for planar perovskite solar cells: Progress and prospective," *Nano Energy*, vol. 68, Feb. 2020, Art. no. 104289.
[34] S. Wenger, S. Seyrling, A. N. Tiwari, and M. Grätzel, "Fabrication and performance of a monolithic dye-sensitized TiO_2/Cu(in,Ga)Se_2 thin film tandem solar cell," *Appl. Phys. Lett.*, vol. 94, no. 17, Apr. 2009, Art. no. 173508.
[35] V. Rondan-Gómez, F. Ayala-Mató, D. Seuret-Jiménez, G. Santana-Rodríguez, A. Zamudio-Lara, I. M. De Los Santos, and H. Y. Seuret-Hernández, "New architecture in dye sensitized solar cells: A SCAPS-1D simulation study," *Opt. Quantum Electron.*, vol. 52, no. 6, pp. 1–11, Jun. 2020.
[36] S. K. Behura, S. Nayak, I. Mukhopadhyay, and O. Jani, "Junction characteristics of chemically-derived graphene/p-Si heterojunction solar cell," *Carbon*, vol. 67, pp. 766–774, Feb. 2014.
[37] P. Chelvanathan, M. I. Hossain, and N. Amin, "Performance analysis of copper–indium–gallium–diselenide (CIGS) solar cells with various buffer layers by SCAPS," *Current Appl. Phys.*, vol. 10, no. 3, pp. S387–S391, May 2010.
[38] F. Wang, Y. Jiang, X. Huang, Q. Liu, Y. Zhang, W. Luo, F. Zhang, P. Zhou, J. Lin, and H. Zhang, "Pro-inflammatory cytokine TNF-α attenuates BMP9-induced Osteo/odontoblastic differentiation of the stem cells of dental apical papilla (SCAPs)," *Cellular Physiol. Biochemistry*, vol. 41, no. 5, pp. 1725–1735, 2017.
[39] F. Anwar, S. Afrin, S. S. Satter, R. Mahbub, and S. M. Ullah, "Simulation and performance study of nanowire CdS/CdTe solar cell," *Int. J. Renew. Energy Res.*, vol. 7, no. 2, pp. 885–893, 2017.
[40] K. Tan, P. Lin, G. Wang, Y. Liu, Z. Xu, and Y. Lin, "Controllable design of solid-state perovskite solar cells by SCAPS device simulation," *Solid-State Electron.*, vol. 126, pp. 75–80, Dec. 2016.
[41] A. K. Kang, M. H. Zandi, and N. E. Gorji, "Simulation analysis of graphene contacted perovskite solar cells using SCAPS-1D," *Opt. Quantum Electron.*, vol. 51, no. 4, pp. 1–9, Apr. 2019.
[42] S. Abdelaziz, A. Zekry, A. Shaker, and M. Abouelatta, "Investigating the performance of formamidinium tin-based perovskite solar cell by SCAPS device simulation," *Opt. Mater.*, vol. 101, Mar. 2020, Art. no. 109738.
[43] M. Minbashi, M. K. Omrani, N. Memarian, and D.-H. Kim, "Comparison of theoretical and experimental results for band-gap-graded CZTSSe solar cell," *Current Appl. Phys.*, vol. 17, no. 10, pp. 1238–1243, Oct. 2017.
[44] J. Verschraegen and M. Burgelman, "Numerical modeling of intra-band tunneling for heterojunction solar cells in SCAPS," *Thin Solid Films*, vol. 515, no. 15, pp. 6276–6279, May 2007.
[45] H. Luo, X. Lin, X. Hou, L. Pan, S. Huang, and X. Chen, "Efficient and air-stable planar perovskite solar cells formed on graphene-oxide-modified PEDOT:PSS hole transport layer," *Nano-Micro Lett.*, vol. 9, no. 4, p. 39, 2017.
[46] S. A. Moiz, A. N. M. Alahmadi, and A. J. Aljohani, "Design of silicon nanowire array for PEDOT:PSS-silicon nanowire-based hybrid solar cell," *Energies*, vol. 13, no. 15, p. 3797, Jul. 2020.

[47] A. M. Nardes, M. Kemerink, R. A. Janssen, J. A. Bastiaansen, N. M. Kiggen, B. M. Langeveld, A. J. Van Breemen, and M. M. De Kok, "Microscopic understanding of the anisotropic conductivity of PEDOT:PSS thin films," *Adv. Mater.*, vol. 19, no. 9, pp. 1196–1200, 2007.

[48] R. Brendel and H. J. Queisser, "On the thickness dependence of open circuit voltages of p-n junction solar cells," *Sol. Energy Mater. Sol. Cells*, vol. 29, no. 4, pp. 397–401, May 1993.

[49] S. A. Moiz, A. N. M. Alahmadi, and K. S. Karimov, "Improved organic solar cell by incorporating silver nanoparticles embedded polyaniline as buffer layer," *Solid-State Electron.*, vol. 163, Jan. 2020, Art. no. 107658.

[50] H. Shi, C. Liu, Q. Jiang, and J. Xu, "Effective approaches to improve the electrical conductivity of PEDOT:PSS: A review," *Adv. Electron. Mater.*, vol. 1, no. 4, 2015, Art. no. 1500017.

[51] S. A. Moiz, I. A. Khan, W. A. Younis, M. I. Masud, Y. Ismail, and Y. M. Khawaja, "Solvent induced charge transport mechanism for conducting polymer at higher temperature," *Mater. Res. Exp.*, vol. 7, no. 9, Sep. 2020, Art. no. 095304.

[52] M. M. Ahmed, K. S. Karimov, and S. A. Moiz, "Temperature-dependent I–V characteristics of organic–inorganic heterojunction diodes," *IEEE Trans. Electron Devices*, vol. 51, no. 1, pp. 121–126, Jan. 2004.

[53] S. A. Moiz, A. M. Nahhas, H.-D. Um, S.-W. Jee, H. K. Cho, S.-W. Kim, and J.-H. Lee, "A stamped PEDOT:PSS–silicon nanowire hybrid solar cell," *Nanotechnology*, vol. 23, no. 14, 2012, Art. no. 145401.

[54] J. Ouyang, "'Secondary doping' methods to significantly enhance the conductivity of PEDOT:PSS for its application as transparent electrode of optoelectronic devices," *Displays*, vol. 34, no. 5, pp. 423–436, 2013.

[55] S. Lee, D. C. Paine, and K. K. Gleason, "Heavily doped poly (3, 4-ethylenedioxythiophene) thin films with high carrier mobility deposited using oxidative CVD: Conductivity stability and carrier transport," *Adv. Funct. Mater.*, vol. 24, no. 45, pp. 7187–7196, 2014.

[56] M. Koopmans, M. A. Leivisk, J. Liu, J. Dong, L. Qiu, J. C. Hummelen, G. Portale, M. C. Heiber, and L. J. A. Koster, "Electrical conductivity of doped organic semiconductors limited by carrier–carrier interactions," *ACS Appl. Mater. Interfaces*, Dec. 2020.

[57] Y. Wang, J. Song, W. Song, Y. Tian, B. Han, X. Meng, F. Yang, Y. Ding, and J. Li, "Effects of thickness on photoelectric properties and perovskite solar cells application of transparent conductive F and Al co-doped ZnO films," *Sol. Energy*, vol. 186, pp. 126–135, Jul. 2019.

[58] W. Hu, S. Yang, and S. Yang, "Surface modification of TiO_2 for perovskite solar cells," *Trends Chem.*, vol. 2, no. 2, pp. 148–162, Feb. 2020.

[59] H.-D. Um, S. A. Moiz, K.-T. Park, J.-Y. Jung, S.-W. Jee, C. H. Ahn, D. C. Kim, H. K. Cho, D.-W. Kim, and J.-H. Lee, "Highly selective spectral response with enhanced responsivity of n-ZnO/p-Si radial heterojunction nanowire photodiodes," *Appl. Phys. Lett.*, vol. 98, no. 3, Jan. 2011, Art. no. 033102.

[60] D. G. Lee, M.-C. Kim, B. J. Kim, D. H. Kim, S. M. Lee, M. Choi, S. Lee, and H. S. Jung, "Effect of TiO_2 particle size and layer thickness on mesoscopic perovskite solar cells," *Appl. Surf. Sci.*, vol. 477, pp. 131–136, May 2019.

[61] P. Wang, Y. Zhao, and T. Wang, "Recent progress and prospects of integrated perovskite/organic solar cells," *Appl. Phys. Rev.*, vol. 7, no. 3, Sep. 2020, Art. no. 031303.

[62] M. Daboczi, I. Hamilton, S. Xu, J. Luke, S. Limbu, J. Lee, M. A. McLachlan, K. Lee, J. R. Durrant, I. D. Baikie, and J.-S. Kim, "Origin of open-circuit voltage losses in perovskite solar cells investigated by surface photovoltage measurement," *ACS Appl. Mater. Interface*, vol. 11, no. 50, pp. 46808–46817, Dec. 2019.

[63] M. Daboczi, J. Kim, J. Lee, H. Kang, I. Hamilton, C. Lin, S. D. Dimitrov, M. A. McLachlan, K. Lee, J. R. Durrant, and J. Kim, "Towards efficient integrated perovskite/organic bulk heterojunction solar cells: Interfacial energetic requirement to reduce charge carrier recombination losses," *Adv. Funct. Mater.*, vol. 30, no. 25, Jun. 2020, Art. no. 2001482.

[64] T. S. Sherkar, C. Momblona, L. Gil-Escrig, J. Ávila, M. Sessolo, H. J. Bolink, and L. J. A. Koster, "Recombination in perovskite solar cells: Significance of grain boundaries, interface traps, and defect ions," *ACS Energy Lett.*, vol. 2, no. 5, pp. 1214–1222, May 2017.

[65] W. Zhao, Z. Yao, F. Yu, D. Yang, and S. Liu, "Alkali metal doping for improved $CH_3NH_3PbI_3$ perovskite solar cells," *Adv. Sci.*, vol. 5, no. 2, 2018, Art. no. 1700131.

[66] E. Socie, B. R. C. Vale, A. Burgos-Caminal, and J. Moser, "Direct observation of shallow trap states in thermal equilibrium with band-edge excitons in strongly confined $CsPbBr_3$ perovskite nanoplatelets," *Adv. Opt. Mater.*, vol. 9, no. 1, Jan. 2021, Art. no. 2001308.

[67] N. Wu, Y. Wu, D. Walter, H. Shen, T. Duong, D. Grant, C. Barugkin, X. Fu, J. Peng, T. White, K. Catchpole, and K. Weber, "Identifying the cause of voltage and fill factor losses in perovskite solar cells by using luminescence measurements," *Energy Technol.*, vol. 5, no. 10, pp. 1827–1835, Oct. 2017.

SYED ABDUL MOIZ received the B.S. degree in computer engineering and the M.S. degree in power engineering from NED University, in 1995 and 1997, respectively, and the Ph.D. degree from the Ghulam Ishaq Khan Institute of Engineering Science and Technology, in 2004. He is currently working as a Professor of Electrical Engineering with the Department of Engineering and Islamic Architecture, Umm Al-Qura University, Saudi Arabia. Before joining Umm Al-Qura University, he worked as a Research Professor with the Semiconductor Nano-Processing Laboratory (SNPL), Hanyang University, South Korea. He worked nearly ten years in Pakistan Atomic Energy Commission as a Professional Engineer. He has authored one book and more than 100 scientific papers in the peer-reviewed international journals and conferences. He was awarded a medal of honour by the Government of Pakistan on the recognition of his contributions. He was also awarded many times as the best teacher during his professional academic career.

A. N. M. Alahmadi received the B.Sc. degree in electronics and communication engineering from King Abdulaziz University, Saudi Arabia, in 2001, and the M.Sc. and Ph.D. degrees in microelectronics from Newcastle University, in 2007 and 2012, respectively. He is currently an Assistant Professor with the Electrical Engineering Department, Umm Al-Qura University. His research interests include design, fabrication, and characterisation of electronic circuits and devices.

ABDULAH JEZA ALJOHANI (Senior Member, IEEE) received the B.Sc. (Eng.) degree in electronics and communication engineering from King Abdulaziz University, Jeddah, Saudi Arabia, in 2006, and the M.Sc. degree (Hons.) and the Ph.D. degree, awarded with no corrections, in wireless communication from the University of Southampton, Southampton, U.K., in 2010 and 2016, respectively. He is currently an Associate Professor with the Department of Electrical and Computer Engineering, King Abdulaziz University. His research interests include machine learning and optimization, distributed source coding, free-space optical communication, channel coding, cooperative communications, and MIMO systems.